First-principles calculations of the magnetic properties of YMn_2 and its hydrides

1996 J. Phys.: Condens. Matter 8 3373

(http://iopscience.iop.org/0953-8984/8/19/012)

J. Phys.: Condens. Matter **8** (1996) 3373–3384. Printed in the UK

First-principles calculations of the magnetic properties of YMn_2 and its hydrides

M Pajda†, R Ahuja‡, B Johansson‡, J M Wills§, H Figiel†, A Paja† and O Eriksson‡

† Faculty of Physics and Nuclear Techniques, University of Mining and Metallurgy, 30-059 Krakow, Alica Mickiewicza 30, Poland

‡ Condensed Matter Theory Group, Physics Department, Uppsala University, S-75121 Uppsala, Sweden

§ Theoretical Division, Los Alamos National Laboratory, Los Alamos, NM 87544, USA

Received 15 December 1995

Abstract. Self-consistent, general potential, electronic structure calculations have been performed for the Laves phase compound YMn_2 and its hydrides YMn_2H_x ($x = 0.5$ and 1.0). The parent material, YMn_2, is found to be an itinerant antiferromagnet with a magnetic moment of $2.6\mu_B$ per Mn atom whereas for the hydrides an additional ferrimagnetic component appears. This is in good agreement with experiment. The dependence of the calculated atom-projected magnetic moments and hyperfine fields on the Mn–H interaction is analysed. We have also calculated the total energy for three different H positions and established that the lowest energy is found for the experimentally observed position.

1. Introduction

The intermetallic compound YMn_2 crystallizes in the C15 structure (the cubic Laves phase). This structure has space group $F4_1/d\bar{3}2m/m$ (O_h^7) and is an fcc-based structure. The unit cell includes four atoms of Mn at 16d ($\bar{3}m$) positions and two atoms of Y at 8a ($\bar{4}3m$) positions [1]. Early studies suggested YMn_2 to be a Pauli paramagnet with a temperature-independent susceptibility. However, it has been shown by neutron diffraction measurements that this compound is an antiferromagnet with a Néel temperature, T_N, of about 100 K [2]. The observed magnitude of the Mn sublattice moment is $2.7\mu_B$ per atom [2]. Upon hydrogenation (YMn_2H_x) a change of the magnetic properties was observed. Moreover, the lattice constant increases with hydrogen content, x, whereas the positions of the Y and Mn atoms were found to remain the same [3]. In hydrogenated YMn_2 the hydrogen atoms are predominantly located at tetragonal sites called A2B2 [3]. More precise, temperature-dependent measurements [4] showed the appearance of a tetragonal distortion for compounds with small concentrations of hydrogen (up to $x = 1.0$) as well as for the parent compound, YMn_2, below 100 K. The tetragonal distortion disappears as the hydrogenation increases. Moreover, in hydrogenated YMn_2 a ferrimagnetic component is observed and the magnetization reaches a value of $0.3\mu_B$ per Mn atom. This was found by Buschow and Sherwood [5] and Fujii *et al* [6] for $x = 3.0$, under the assumption that Y had no magnetic moment.

On the theoretical side the electronic structure and magnetic moments have been calculated for YMn_2 [7] using a tight-binding Hartree–Fock method, but no energy band

0953-8984/96/193373+12$19.50

calculations have been reported for the hydrides. As pointed out in [5] and [6] this is highly desired in order to explain the experimental findings. The interesting experimental data on hydrogenated YMn_2, discussed above, have thus motivated us to investigate this material by means of first-principles electronic structure calculations.

2. Calculational details

2.1. The full-potential LMTO technique

Our theoretical approach is based on the local density approximation (with the von Barth–Hedin parametrization) of density functional theory. The Kohn–Sham equation was solved by means of a full-potential linear muffin-tin orbital technique [8]. The calculations were scalar relativistic (without spin–orbit coupling) and employed no shape approximation to the charge density and potential. The basic geometry of the potential was chosen as non-overlapping muffin tins with a true interstitial region. The basis functions, charge density, and potential were expanded in spherical harmonic series inside the muffin tins and in a Fourier series in the interstitial. The basis set contained 4d, 5s, and 5p orbitals for Y, 3d, 4s, and 4p orbitals for Mn, and 1s states for H. All orbitals were contained in the same energy panel. Integration over the Brillouin zone was done using 'special-point' sampling [9, 10] and self-consistency was obtained with 172 $\boldsymbol{k}$-points in the irreducible wedge of the Brillouin zone. The muffin-tin sphere radii were chosen to have the ratios 1:0.71:0.36 between the Y, Mn, and H atoms. The calculated results (total energy and magnetic moments) are typically rather insensitive to this choice. However, the different types of expansion (Fourier series in the interstitial and spherical harmonics inside the muffin-tin spheres) can be made to converge more quickly if a proper base geometry is chosen. The above-mentioned ratios between different muffin-tin spheres were found to give rise to well converged expansions. Moreover, the calculations were performed for the experimentally determined lattice constants [6] as well as for the experimentally observed atomic positions [11].

2.2. The choice of primitive cell

For pure YMn_2 the primitive cell was chosen to have six atoms: two different types of Y (a total of two Y atoms) and two different types of Mn (a total of four Mn atoms). In this case the number of point group operations of the lattice amounts to 4. The spherical harmonic expansions were carried out through to $l = 4$ for the basis functions, charge density, and potential. Putting the hydrogen atoms into YMn_2 causes a further lowering of the symmetry. Hydrogen occupying A2B2 sites has 24 choices (this is the total number of crystallographic positions of A2B2 type per primitive unit cell) whereas we wish to have occupation of only one or two of them, corresponding to hydrogen concentrations of 0.5 and 1.0, respectively. In this case there is no symmetry in the system except the identity operation and there are four different Mn atoms and two different Y atoms.

3. Results

3.1. Paramagnetic results

The density of states (DOS) for paramagnetic YMn_2H_x ($x = 0.5$ and 1.0) is presented in figure 1, to be compared with the corresponding plot of YMn_2 (shown at the top of figure 1).

Table 1. Calculated magnetic moments on the different types of atom (labelled with numbers 1 and 2 for Y and 1–4 for Mn) in the compounds YMn_2H_x ($x = 0.0$, 0.5, 1.0). $\langle$Mn$\rangle$ denotes the average of the magnitudes of the different Mn atoms, Mn_{exp} is the experimental Mn moment. M and M_{exp} represent the theoretical and experimental net magnetization per Mn atom, respectively. The superscripts a and b on YMn_2 denote moments of YMn_2 at volumes corresponding to $YMn_2H_{0.5}$ and $YMn_2H_{1.0}$, respectively.

	Y1	Y2	Mn1	Mn2	Mn3	Mn4	$\langle$Mn$\rangle$	Mn_{exp}	M	M_{exp}
YMn_2	0.00	0.00	2.61	−2.61	—	—	2.61	2.7	0.0	0.0
$YMn_2H_{0.5}$	0.02	0.02	2.82	−2.42	−2.42	2.82	2.62	—	0.2	—
$YMn_2H_{1.0}$	0.03	0.03	3.02	−2.59	−2.26	2.63	2.62	—	0.2	0.1
YMn_2^a	0.00	0.00	2.81	−2.81	—	—	2.81	—	0.0	0.0
YMn_2^b	0.00	0.00	2.92	−2.92	—	—	2.92	—	0.0	0.0

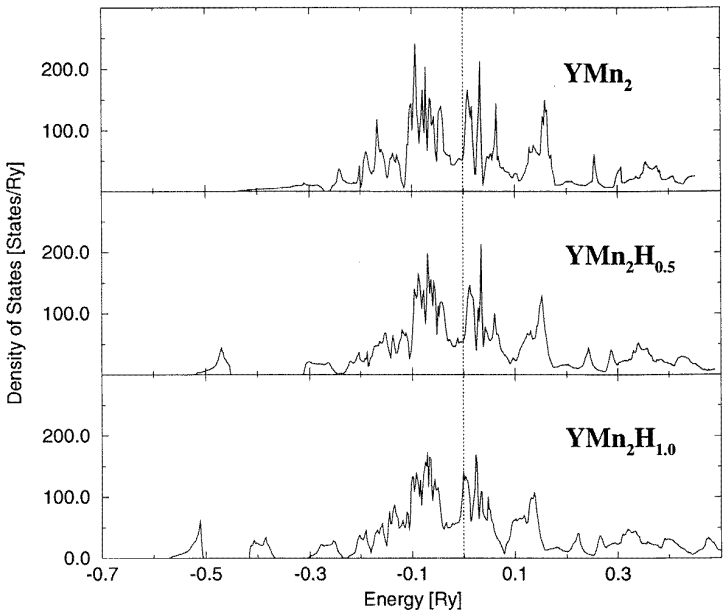

Figure 1. Paramagnetic densities of states for YMn_2 (top), $YMn_2H_{0.5}$ (middle), and $YMn_2H_{1.0}$ (bottom). The Fermi energy is at zero and energy is in rydbergs.

The DOS for all systems have approximately the same shape. However, along with the increase of hydrogen concentration a modification of the DOS appears for lower energies, and more importantly there are additional contributions between approximately -0.6 and -0.3 Ryd, which come mostly from the s band of hydrogen. For pure YMn_2 the position of the Fermi level (E_F) is near a minimum of the DOS. This fact suggests that YMn_2 should not become ferromagnetic. As the hydrogen content increases, the Fermi level (E_F) shifts slightly upwards, so the DOS at the Fermi level $D(E_F)$ increases, which is an indication of the possibility of ferromagnetism. Part of the reason for the change in the position of E_F is that the volume of the system increases with the H content. However, H also induces a redistribution of the electron states. A glance at the following plots (figures 2–4),

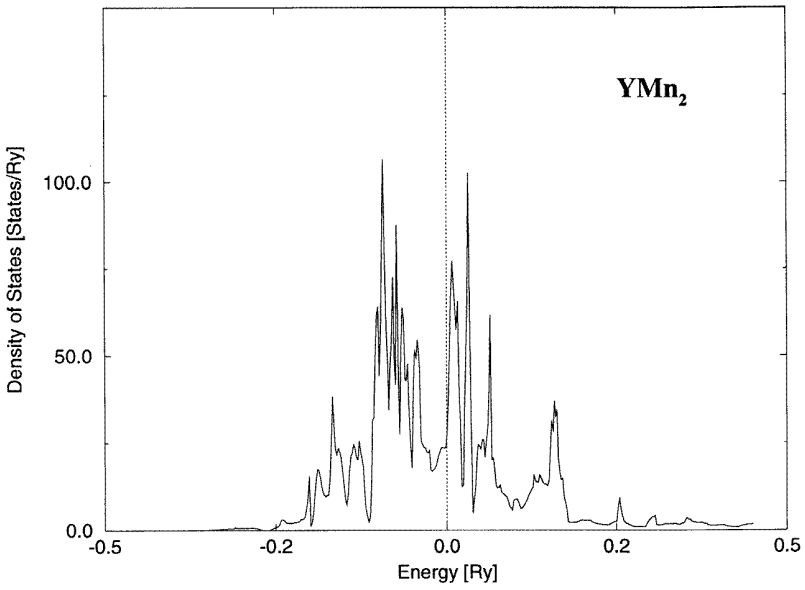

Figure 2. The projection of the paramagnetic density of states for YMn_2 on the d orbital of the Mn sites. The Fermi energy is at zero and energy is in rydbergs.

representing the H- and Mn-projected DOS, shows this effect and we discuss it in some detail below. For YMn_2 the projected DOS are identical for both types of Mn atom and for this reason we show only one of them (figure 2). For $YMn_2H_{0.5}$ we distinguish two different Mn DOS (figure 3). This is connected with the fact that the distance between the hydrogen atom and the different Mn atoms is different, such that two Mn atoms lie closer to the H atom and two Mn atoms lie further away from the H atom. The low-energy part of the Mn DOS is slightly modified by the presence of the hydrogen atoms. However, most features of the Mn d states remain relatively unchanged in the presence of hydrogen (compare with figure 2). Putting additional hydrogen in the system ($YMn_2H_{1.0}$—figure 4) causes a further enhancement of the difference between the various Mn atoms, and now we isolate four different types of Mn DOS. We note that there are two different H-projected DOS but since they are very similar we show only one of them. Also for YMn_2H_1 the gross features of the Mn 3d DOS are relatively little changed. The largest modification is found in the low-energy region where the Mn–H hybridization induces a change in the Mn d DOS. Since the H 1s states are located at lower energies in both $YMn_2H_{0.5}$ and $YMn_2H_{1.0}$, one would naively expect a charge transfer from Mn and Y to the H atom. However, the Y and Mn DOS are more or less unchanged with respect to H entering the material, and since E_F moves slightly upwards with increasing H concentration this suggests that H acts as an electron donor. In fact, neither of these extremes is found in YMn_2, since the calculated occupation numbers of the Y and Mn atoms change only marginally upon hydrogenation. Instead, as seen in the DOS plots, in the low-energy interval there is strong hybridization between the H 1s states and the orbitals centred on the Y and Mn atoms. We make a final comment on the paramagnetic calculations: the H-projected DOS is quite different for $YMn_2H_{0.5}$ and YMn_2H_1. The H s band thus does not act as a rigid level in this system but changes its dispersion and energy depending on the H concentration.

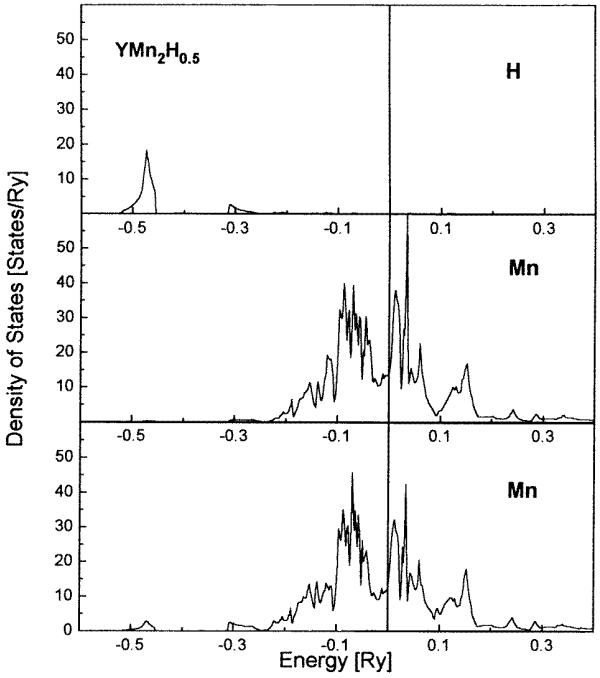

Figure 3. The projection of the paramagnetic density of states for $YMn_2H_{0.5}$ on the d orbital of the two different Mn sites and on the s orbital for the H atom. The Fermi energy is at zero and energy is in rydbergs.

3.2. Spin-polarized results

Next, we performed spin-polarized calculations, and the spin magnetic moments obtained are presented in table 1. In these calculations we found that an antiferromagnetic ground state had the lowest energy as compared to a paramagnetic or a ferromagnetic one, in good agreement with experiment. It should be pointed out, however, that the experimental antiferromagnetic state is a little more complex with a non-collinear ordering of the moments on the Mn sites. The theoretical value of the magnetic moment on the different Mn atoms in pure YMn_2 agrees almost perfectly with data from neutron scattering experiments, and amounts to $2.6\mu_B$. This is also in agreement with the tight-binding, Hartree–Fock calculations of [7]. For the hydrides the situation is more complicated. Let us first consider the values of the magnetic moments on the Mn atoms in $YMn_2H_{0.5}$. We see from table 1 that they are bigger on two of the atoms (which we have numbered 1 and 4) and smaller on the other two atoms (numbered 2 and 3). The Mn atoms with the lowest moments are geometrically closer to the H atoms and the Mn–H hybridization is strongest for these atoms (figure 3). However, the average value of the magnitude of the magnetic moments for all four Mn atoms is quite similar to that for the parent compound. A similar situation is found for $YMn_2H_{1.0}$ since on those Mn atoms where hybridization with the hydrogen is stronger the value of the magnetic moment is reduced. In contrast, on those atoms where hybridization with the H is weaker the moment is enlarged. To exemplify this, we observe in table 1, for $YMn_2H_{1.0}$, that one Mn moment is quite small ($2.26\mu_B$), two Mn moments have intermediate size ($\approx 2.6\mu_B$) and one Mn moment is large ($3.02\mu_B$). This correlates roughly

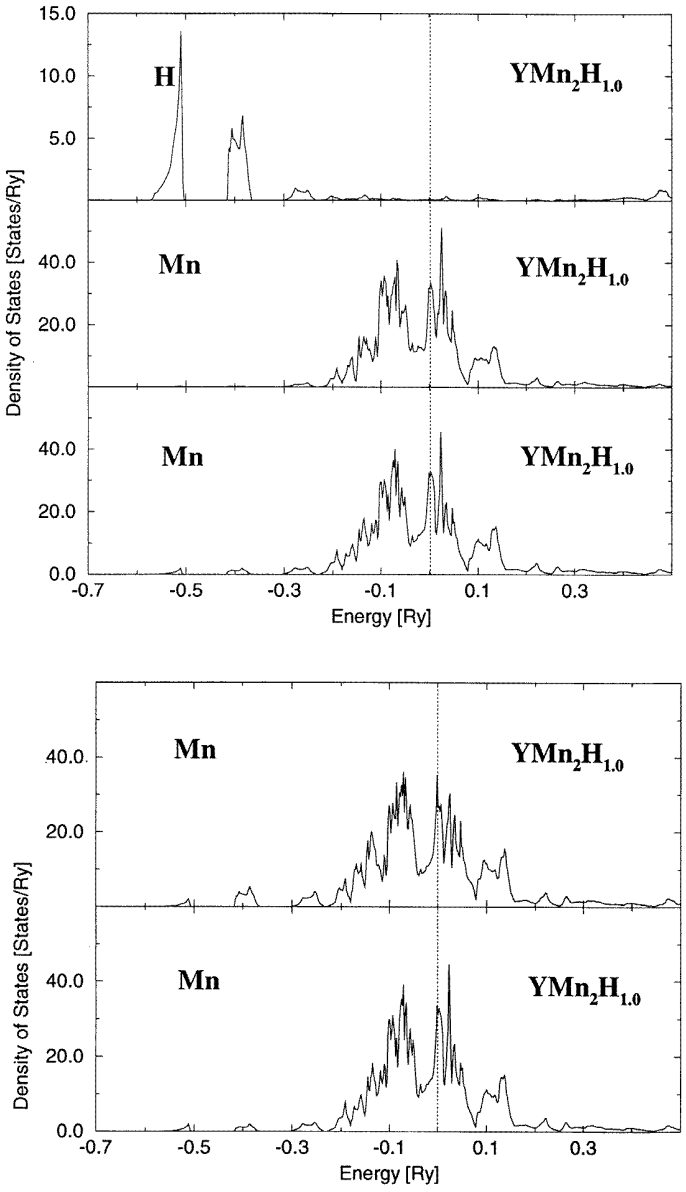

Figure 4. The projection of the paramagnetic density of states for $YMn_2H_{1.0}$ on the d orbital of four different Mn sites and on the s orbital of the H atom. The Fermi energy is at zero and the energy is in rydbergs.

with the Mn–H hybridization seen from the DOS plot in figure 4. This figure shows that the H–Mn hybridization is large for one atom, intermediate for two atoms, and small for the last one. This is most clearly seen in the features of the Mn DOS in the energy interval between -0.6 and -0.3 Ryd. Thus there is a connection between strong Mn–H hybridization and reduced magnetism in this system. Also for $YMn_2H_{1.0}$ the average of the magnitude of the moments is close to the value for YMn_2 (table 1). In order to show that the change

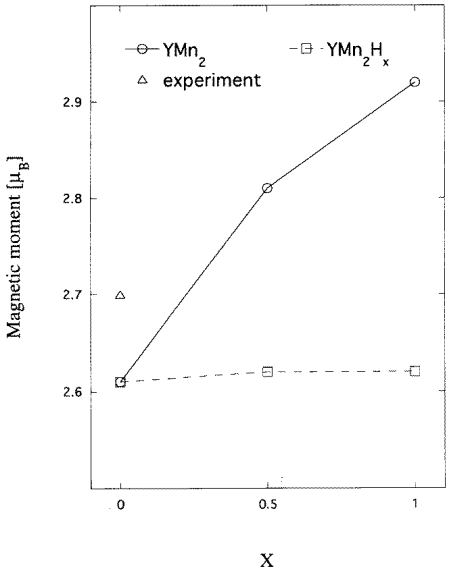

Figure 5. The calculated average magnetic moment for YMn_2H_x of the Mn atoms versus hydrogen concentration (squares). Open circles denote magnetic moments on Mn atoms for YMn_2 assuming a unit-cell volume corresponding to the hydrides with $x = 0.5$ and 1.0. Experimental data are indicated with triangles.

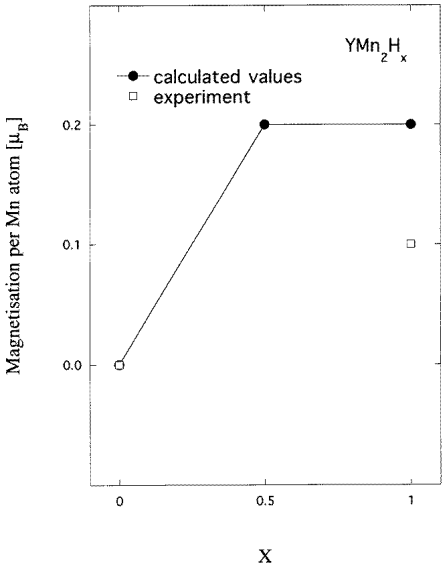

Figure 6. Magnetization per Mn atom versus hydrogen concentration for YMn_2H_x.

of the Mn magnetic moments upon hydrogenation is not only caused by the modification of the volume but also by the influence of hydrogen on the electronic structure, we carried out calculations for pure YMn_2 at volumes corresponding to $YMn_2H_{0.5}$ and $YMn_2H_{1.0}$. As may be deduced from table 1 the increased volume of YMn_2 leads to an increase of the

magnetic moment of the Mn atoms, with no influence on the type of magnetic order (the system is still antiferromagnetic). This behaviour of Mn is characteristic for compounds with rare-earth elements and was discussed elsewhere [7]. If we compare the Mn moments of YMn_2H_x with the Mn moments for the corresponding volumes of YMn_2 we observe that the presence of hydrogen reduces the magnetic moments for all Mn atoms except the one which we have denoted Mn1. For this atom there is, surprisingly, a slightly increased magnetic moment of the hydrated compound as compared to the parent compound with a similar volume. This fact holds both for a hydrogen concentration, x, of 0.5 and one of 1.0. In figure 5 we compare the average of the magnitude of the Mn moment of YMn_2H_x with the magnitude of the Mn moments of YMn_2, for volumes corresponding to the hydrogenated system. Here it is clear that isolating the effect of the increased volume causes the Mn moment to increase, as expected. However, the tendency of the moments to become larger with increasing volume (due to the hydrogen uptake) is compensated by the influence that the hydrogen atoms have on the electronic structure (hybridization with the Mn atoms). The net result is an almost constant behaviour of the moment, as seen in figure 5.

Table 2. Calculated hyperfine fields in tesla on the different atom types in YMn_2. $\langle$Mn$\rangle$ represents the average of the magnitudes at the different Mn atoms. $|Mn_{exp}|$ is the magnitude of the experimental value for Mn.

	Y1	Y2	Mn1	Mn2	Mn3	Mn4	$\langle$Mn$\rangle$	$\lvert Mn_{exp}\rvert$
B_{val}	−0.16	−0.16	31.22	−31.22	—	—	—	—
B_{core}	0.14	0.14	−44.62	44.62	—	—	—	—
B_{tot}	−0.02	−0.02	−13.4	13.4	—	—	13.4	12.1

Table 3. Calculated hyperfine fields on the different atom types in $YMn_2H_{0.5}$. $\langle$Mn$\rangle$ represents the average of the magnitudes at the different Mn atoms. $|Mn_{exp}|$ is the corresponding magnitude of the experimental value for Mn.

	Y1	Y2	Mn1	Mn2	Mn3	Mn4	$\langle$Mn$\rangle$	$\lvert Mn_{exp}\rvert$
B_{val}	−1.71	−3.51	29.93	−23.87	−23.87	29.09	—	—
B_{core}	1.34	1.59	−43.23	36.28	36.27	−42.91	—	—
B_{tot}	−0.37	−1.92	−13.3	12.4	12.4	−13.81	13.0	—

The presence of hydrogen at A2B2 positions gives an additional result, namely the appearance of a non-zero net magnetization, which is almost the same for the two hydrogen concentrations studied here ($x = 0.5$ and 1.0). The magnetic moment amounts approximately to $0.2\mu_B$ per Mn atom (figure 6). This result is in acceptable agreement with experiment. Fujiwara [12] measured $0.19\mu_B$ per Mn atom for $YMn_2H_{2.4}$ and Fujii *et al* [6] measured $0.1\mu_B$ for $YMn_2H_{1.0}$. We wish to underline that in our calculations, the choice of the hydrogen positions using the experimental data (A2B2 position) is of crucial importance for obtaining this result. For comparison, we also calculated the magnetic moments and the magnetization for the hydrides for another possible atomic position (the tetragonal B4 site), which has higher symmetry. This tetragonal position is in the very middle of tetrahedra spanned by four Mn atoms. Thus the distances between the hydrogen atom and all four Mn atoms in the tetrahedron are equal to each other. We obtained in this case a decreasing magnetic moment on each Mn atom when the hydrogen content increases and a zero net magnetization for the system. Also, the total energy for this H position was substantially

higher than for the A2B2 position. We also calculated the total energy for a third H position called AB3. In this location the H is surrounded by three nearest-neighbouring Mn atoms and one Y atom. The total energy for this configuration is only slightly larger (∼4 mRyd/H atom) than for the A2B2 geometry.

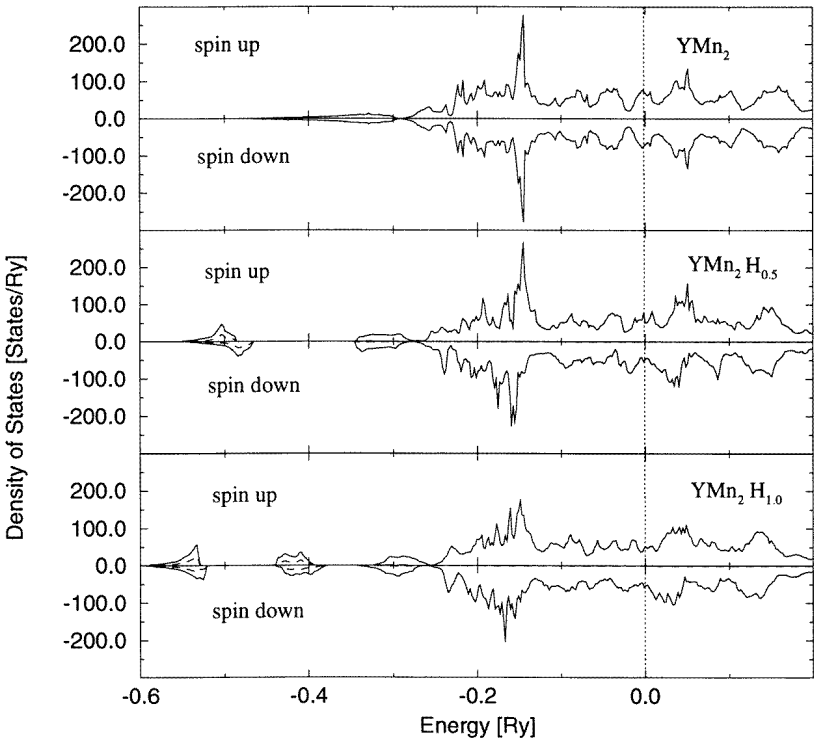

Figure 7. Spin-polarized densities of states for YMn_2, $YMn_2H_{0.5}$, and $YMn_2H_{1.0}$. The solid lines represent the total densities of states and the dashed lines represent the hydrogen contributions. The Fermi level is at zero and the energy is in rydbergs.

The total DOS for spin-polarized YMn_2 (figure 7—top panel) is symmetric for the spin-up and spin-down states, which is typical for antiferromagnetic ordering of spins. This symmetry is broken by hydrogenation which, as mentioned, causes the appearance of a ferrimagnetic component. This may be seen in the DOS plots for $YMn_2H_{0.5}$ and $YMn_2H_{1.0}$ (middle and bottom panels of figure 7). The dashed lines of the DOS plots of the hydrides represent the hydrogen 1s DOS. Note also that the H 1s states have an exchange splitting and the corresponding H magnetic moments are $\sim 0.03\ \mu_B$/H atom for both $YMn_2H_{0.5}$ and $YMn_2H_{1.0}$. Notice also in figure 7 that the main features of the DOS are rather insensitive to the H concentration, as was also found for the paramagnetic calculation (figure 1).

3.3. Hyperfine fields

The hyperfine field, $\boldsymbol{B}_{hf}$, in the absence of an external field, can be separated into three different contributions [13]: the magnetic dipole term, the orbital momentum term and the Fermi contact term. In 3d elements the orbital term is small because the expectation value

Table 4. Calculated hyperfine fields on the different atom types in $YMn_2H_{1.0}$. ⟨Mn⟩ represents the average of the magnitudes at the different Mn atoms. $|Mn_{exp}|$ is the corresponding magnitude of the experimental value for Mn.

	Y1	Y2	Mn1	Mn2	Mn3	Mn4	⟨Mn⟩	$\|Mn_{exp}\|$
B_{val}	−0.98	−0.68	33.38	−25.98	−22.83	26.42	—	—
B_{core}	1.28	1.04	−46.73	39.19	34.15	−39.43	—	—
B_{tot}	0.3	0.41	−13.35	13.21	11.31	−13.29	12.79	12.4

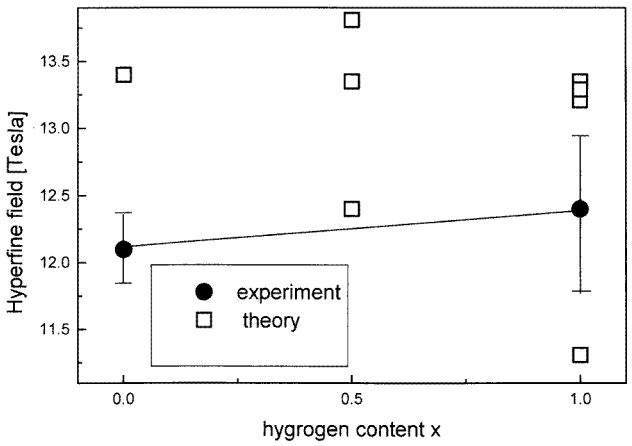

Figure 8. The calculated (open squares) and experimental (solid circle) hyperfine field on the Mn atoms versus hydrogen concentration for YMn_2H_x.

$\langle L_z \rangle$ is, to a large extent, quenched by the crystalline field [14]. Since the classical dipolar term is expected to be small as well, we concentrate on the Fermi contact term. This quantity is given by the expression [15]

$$B_{hf} = \frac{8\pi}{3}\frac{eh}{2mc}[\rho^{\uparrow}(0) - \rho^{\downarrow}(0)] \approx 54\sum_i [|\psi_i^{\uparrow}(0)|^2 - |\psi_i^{\downarrow}(0)|^2].$$

In this equation e is the electron charge, h is Planck's constant, m is the electron mass and c is the speed of light. Furthermore, $\rho^{\uparrow}$ is the spin-up charge density and ψ_i is the wave function for orbital i. Thus each orbital contributes an amount proportional to its spin density at the origin. This expression contains both a core and a valence contribution. In the case of Mn the core contribution consists of 1s, 2s, and 3s orbitals and the valence contribution consists of a 4s orbital. The spin contact density was calculated from our first radial mesh point, which is taken very close to the nuclear radius. Explicit tests showed this to be a good approximation for comparing differences in contact densities for different compounds [16]. Our calculated values for the atom-projected hyperfine fields are presented in tables 2–4, for YMn_2, $YMn_2H_{0.5}$, and $YMn_2H_{1.0}$, respectively. As we can see from a comparison between tables 1 and 2–4, there is an approximately linear relationship between the spin moment and the total B_{hf} for a given site. Normally the core contribution to the hyperfine field is proportional [15] to the magnetic moment, whereas the valence contribution is not. One can also note that the values of the hyperfine fields do not change too much along with the hydrogenation, which is consistent with the fact that the

magnitudes of the moments are rather insensitive to the H content. However, the calculated change in B_{hf} upon hydrogenation is smaller than the corresponding change in magnetic moments (compare table 1 with tables 2–4). Thus, from hyperfine-field measurements one would, assuming a proportionality between B_{hf} and the magnetic moment, underestimate the variation in magnetic moments for the different Mn atoms.

Our theoretical results are to be compared to the experimental data represented by the NMR spectra for YMn_2 and $YMn_2H_{1.0}$ [17, 18] (tables 2–4 and figure 8). Note that the agreement between experiment and theory is acceptable. Moreover, experimentally it is observed, both for YMn_2 and $YMn_2H_{1.0}$, that there is only one frequency peak, corresponding to the value of the hyperfine field on the Mn atom. However, for the hydrides the width of the experimental peak is substantially larger compared to that for the parent material. Based on our calculations, where we find different B_{hf} on the different Mn atoms of the hydrides, we interpret the experimental spectrum as being composed of two or more slightly different values of the hyperfine fields coming from different Mn sites. If this interpretation is correct it still means that the calculations overestimate the difference between the hyperfine fields at different Mn atoms, since the width of the experimental spectrum (for $x = 1$) is $\approx$1 T [17, 18] to be compared to our calculated difference of different Mn atoms of $\approx$2 T. Possibly dynamical effects, involving atomic motion of the H atoms, need to be considered to resolve this issue.

4. Conclusions

In this work we have calculated magnetic moments and the hyperfine field of YMn_2H_x, for x-values ranging between 0 and 1, and obtained acceptable agreement with experimental data. The hydrogenated compound is found to be antiferromagnetic for all concentrations of H, with a small ferrimagnetic component. The calculated net magnetic moment as well as the individual Mn moments are found to be in decent agreement with experimental data. A similar agreement between theory and experiment is found for the hyperfine field. As regards the electronic structure, the H 1s states are found to lie below the Mn d band. Due to strong hybridization between the H 1s orbital and the Mn states (4s and 3d) there is little charge transfer in this system. The Mn–H hybridization is found to reduce the magnetic moment on the Mn site, and there is a correlation between strong hybridization and reduced Mn moment. The influence of the increased volume (due to hydrogenation) and of the Mn–H hybridization on the magnetic properties are investigated and found to be competing. The increased lattice constant produces larger Mn moments whereas the Mn–H hybridization reduces the Mn moments. Finally, we have investigated the energy for three different H positions and found that the experimentally observed A2B2 position had the lowest energy and that the AB3 positions have only marginally higher energy. This fact is consistent with the fact that at elevated temperatures experiments suggest that these two positions are populated by hydrogen [17, 18].

Acknowledgments

OE and BJ are grateful to the Swedish Natural Science Research foundation for financial support. The support from the Materials Consortium 9 is also appreciated.

References

[1] Henry N F M and Lonsdale K 1965 *International Tables for X-Ray Crystallography* vol 1 (Birmingham: Kynoch) p 340
[2] Nakamura Y, Shiga M and Kawano S 1983 *Physica* B **120** 6741
[3] Buschow K H J 1977 *Solid State Commun.* **21** 1031
[4] Cywinski R, Kilkoyne S H and Scott C A 1991 *J. Phys.: Condens. Matter* **3** 6473
[5] Buschow K H J and Sherwood R C 1987 *J. Appl. Phys.* **49** 1480
[6] Fujii H, Saga M and Okamoto T 1987 *J. Less-Common. Met.* **130** 25
[7] Yamada H and Shimizu M 1987 *J. Phys. F: Met. Phys.* **17** 2249
Yamada H, Inoue J, Terao K, Kanda S and Shimizu M 1984 *J. Phys. F: Met. Phys.* **14** 1943
Asano S and Ishida J 1985 *J. Phys. Soc. Japan* **54** 3925
[8] Wills J M and Cooper B R 1987 *Phys. Rev.* B **36** 3809
[9] Chadi D J and Cohen M L 1973 *Phys. Rev.* B **8** 5747
[10] Froyen S 1989 *Phys. Rev.* B **39** 3168
[11] Przewoznik J, unpublished data
[12] Fujiwara K 1988 *J. Phys. Soc. Japan* **57** 2133
[13] Greenwood N N and Gibb T C 1971 *Mössbauer Spectroscopy* (London: Chapman and Hall)
[14] Ashcroft N W and Mermin J 1976 *Solid State Physics* (Philadelphia, PA: Saunders College) pp 657–9
[15] Freeman A J and Watson R 1965 *Magnetism* vol 2A, ed G T Rado and H Suhl (New York: Academic)
[16] Eriksson O and Svane A 1988 *J. Phys.: Condens. Matter* **1** 1589
[17] Kapusta Cz, Przewoznik J, Zukrowski J, Spiridis N, Figiel H and Krop K 1990 *Hyperfine Interact.* **59** 353
[18] Figiel H, Kapusta Cz, Spiridis N, Riedi P C and Lord J S 1993 *Z. Phys. Chem.* **179** 467